

**Full Paper**

**A “cell-friendly” window for the interaction of cells with  
hyaluronic acid/poly-L-lysine multilayers**

Narayanan Madaboosi,<sup>a,b</sup> Katja Uhlig,<sup>a</sup> Stephan Schmidt,<sup>a,c</sup> Anna S. Vikulina,<sup>d</sup> Helmuth  
Möhwald,<sup>b</sup> Claus Duschl,<sup>a</sup> Dmitry V. Volodkin<sup>a,d\*</sup>

---

Dr Narayanan Madaboosi,

<sup>a</sup> Fraunhofer Institute for Cell Therapy and Immunology, Branch Bioanalytics and Bioprocesses (Fraunhofer IZI-BB), Department Cellular Biotechnology & Biochips, Am Mühlenberg 13, 14476 Potsdam-Golm, Germany

<sup>b</sup> Max Planck Institute for Colloids and Interfaces, Am Mühlenberg 1, 14476 Potsdam-Golm, Germany

Dr Katja Uhlig,

<sup>a</sup> Fraunhofer Institute for Cell Therapy and Immunology, Branch Bioanalytics and Bioprocesses (Fraunhofer IZI-BB), Department Cellular Biotechnology & Biochips, Am Mühlenberg 13, 14476 Potsdam-Golm, Germany

Dr Stephan Schmidt,

<sup>b</sup> Max Planck Institute for Colloids and Interfaces, Am Mühlenberg 1, 14476 Potsdam-Golm, Germany

<sup>c</sup> Heinrich-Heine-Universität Düsseldorf, Institut für Organische und Makromolekulare Chemie, Universitätsstr.1, 40225 Düsseldorf, Germany

Dr Anna Vikulina,

<sup>d</sup> School of Science and Technology, Nottingham Trent University, Clifton Lane, Nottingham NG11 8NS, United Kingdom

Prof Helmuth Möhwald,

<sup>b</sup> Max Planck Institute for Colloids and Interfaces, Am Mühlenberg 1, 14476 Potsdam-Golm, Germany

Dr Claus Duschl,

<sup>a</sup> Fraunhofer Institute for Cell Therapy and Immunology, Branch Bioanalytics and Bioprocesses (Fraunhofer IZI-BB), Department Cellular Biotechnology & Biochips, Am Mühlenberg 13, 14476 Potsdam-Golm, Germany

Corresponding author: Prof Assoc Dmitry V. Volodkin,

Email: [dmitry.volodkin@ntu.ac.uk](mailto:dmitry.volodkin@ntu.ac.uk)

<sup>a</sup> Fraunhofer Institute for Cell Therapy and Immunology, Branch Bioanalytics and Bioprocesses (Fraunhofer IZI-BB), Department Cellular Biotechnology & Biochips, Am Mühlenberg 13, 14476 Potsdam-Golm, Germany

<sup>d</sup> School of Science and Technology, Nottingham Trent University, Clifton Lane, Nottingham NG11 8NS, United Kingdom

## **Abstract**

Polyelectrolyte multilayers assembled from hyaluronic acid (HA) and poly-L-lysine (PLL) are most widely studied showing excellent reservoir characteristics to host molecules of diverse nature; however, thick (HA/PLL)<sub>n</sub> films were often found cell-repellent. By a systematic study of the adhesion and proliferation of various cells as a function of bilayer number 'n' a correlation with the mechanical and chemical properties of films is developed. The following cell lines have been studied: mouse 3T3 and L929 fibroblasts, human foreskin primary fibroblasts VH-Fib, human embryonic kidney HEK-293, human bone cell line U-2-OS, Chinese hamster ovary CHO-K and mouse embryonic stem cells. All cells adhere and spread well in a narrow 'cell-friendly' window, identified in the range of n=12-15. At n<12, the film is inhomogeneous and at n>15, the film is cell-repellent for all cell lines. Cellular adhesion correlates with the mechanical properties of the films showing that softer films at higher 'n' number exhibiting a significant decrease of the Young's modulus below 100 kPa are weakly adherent to cells. This trend cannot be reversed even by coating a strong cell-adhesive protein fibronectin onto the film. This indicates that mechanical cues plays a major role for cell behaviour, also in respect to biochemical ones.

## **1. Introduction**

Substantial parts of current research in the field of biomedicine and tissue engineering focus on developing bioactive materials that would efficiently control cell behaviour on their surface. The characterisation of cell behaviour is based on the study of relevant cellular mechanisms and includes processes such as adhesion, spreading, proliferation and migration, of cells. In addition, the understanding of molecular details such as actin polymerization, integrin clustering, signal transduction of cells at interfaces is crucial for the design of biomaterials.<sup>[1, 2]</sup>

Along these lines, the approach to the understanding of cells has begun to expand its horizons from the classical biochemical to biomechanical ones. In this context, the field of mechanobiology has started gaining rapid momentum in recent years, extending its applications to the areas of cell engineering and regenerative medicine.<sup>[3-5]</sup> Such studies pertaining to mechanobiology have gone a long way in exploring concepts related to not only known cellular events but also complex processes like morphodynamics<sup>[6]</sup>, tissue development<sup>[7]</sup> as well as cell-induced stresses<sup>[8]</sup>.

Thus, to understand cell behaviour on surfaces, suitable biomaterials that support enhanced cell growth as well as those that provide flexibility for engineering to tailor the test parameters with conducive features (such as stability, biocompatibility and reservoir features) become attractive. The layer-by-layer (LbL) method introduced for the deposition of PEM films renders simplicity, robustness and versatility in the fabrication process.<sup>[9-12]</sup> Polyelectrolyte multilayers (PEMs) have become immensely popular among biomaterial scientists, as these systems offer a wide range of possibilities to tune their physico-chemical properties and to achieve high reservoir capacity.<sup>[13-16]</sup> The mechanisms of PEM growth and loading with bioactive molecules is, however, still not well understood.<sup>[17-20]</sup> Despite strong attraction of the films from the application point of view, it is found that variation of the film physico-chemical properties significantly influences the behaviour of cells grown on them. Various studies<sup>[21-29]</sup> have been already done to check the response of different cell types on these PEMs. Table ST1 (supporting information) gives an outline of the most significant studies covering PEM-cell interactions. Most of these studies suggest that the film physico-chemical properties have a profound influence on different events related to cellular behaviour, which extends even up to the complex differentiation process. However, there is no systematic study on the effect of cellular response as a function of bilayer number 'n' that is the main variable allowing an effective tuning of the film properties.

In the current study, the model PEM system, hyaluronic acid/poly-L-lysine (HA/PLL) has been exploited to test the behaviour of different cell types in terms of their adhesive, spreading, and proliferative capacities. HA/PLL possesses unique characteristics that distinguish it from other PEM systems, and is one of the most investigated exponential-like growing systems, whose thickness may easily reach micrometer dimensions<sup>[24]</sup> offering perfect reservoir properties for biomacromolecules (proteins, DNA, etc) as well as nano- and microcarriers (liposomes, capsules).<sup>[30-35]</sup> Hence, this system was chosen to test the response of diverse types of cells in a systematic manner by tailoring the PEM properties by the bilayer number 'n'. For the first time, we report a 'cell-friendly window' for HA/PLL films where the films are cell adhesive for all the tested cell lines. This 'window' could be exploited for selective growth, targeted release and other potential studies combining controlled cell growth on the HA/PLL films. Such studies become very essential in order to understand the fundamental aspects of cellular response to soft PEM films and to exploit the films for future biomedical applications.

## **2. Experimental Section**

### **2.1. Materials**

Poly-L-lysine hydrobromide (Mw 24 kDa), poly-L-lysine – FITC labelled (Mw 15-30 kDa), poly(ethyleneimine) (Mw 750 kDa), Poly(allylamine hydrochloride) (Mw 56 kDa), poly(sodium 4-styrenesulfonate) (Mw 70 kDa), Tris base and sodium chloride were purchased from Sigma, Germany and used without further purification. Dried sodium hyaluronate (Mw 360 kDa) was from Lifecore Biomedical, USA and hydrochloric acid from Merck, Germany. The water used in all experiments was prepared in a three-stage Millipore Milli-Q Plus 185 purification system and had a resistivity higher than 18.2 M $\Omega$  cm. The 12mm (diameter) round coverslips (Size No. 1) were purchased from Marienfeld GmbH, Germany and Hellmanex II from Hellma Analytics, Germany.

## 2.2. HA/PLL film fabrication and characterization

The PEM films (HA/PLL)<sub>n</sub>, where 'n' refers to the number of bilayers, were fabricated using a dipping robot, purchased from Riegler and Kirstein GmbH, Germany. The PEs (PLL, HA, PSS, PAH and PEI) were prepared at a concentration of 0.5 mg/ml in film wash buffer (FWB - 10 mM Tris, 15 mM NaCl, adjusted to a pH of 7.2 with 1 M HCl). HA was heated to 60°C for 15-20 min under constant stirring to ensure complete dissolution. The dissolved PEs were filtered through a 0.45 µm syringe filter to remove impurities. The glass coverslips used for deposition were inserted in in-house-designed teflon holders and cleaned by consecutive incubations in hot solutions (60°C) of 2% Hellmanex, 1 M HCl (as Hellmanex is a strong detergent that could not be removed easily by gentle rinsing) and water, under stirring for 15 min in each solution, followed by adequate rinsing with copious amounts of water to remove traces of detergent and acid remaining on the surface. The film build-up was carried out at RT by alternate dipping of the cleaned surfaces in each of the PEs for 10 min, with intermittent rinsing thrice with FWB, each lasting 3 min (thus, totally 9 min between every PE step). An initial coating of PEI, also at the same conditions as other PEs, was done for all the samples before the actual deposition begun.

The CLSM images were obtained using a Leica confocal scanning system mounted onto a Leica Aristoplan and equipped with a 63x oil immersion objective with a numerical aperture of 1.4. The images obtained were analysed using LCS software. Measurement of elastic properties of the HA/PLL film have been performed using the colloidal probe technique as described in <sup>[36]</sup>.

To quantify the amount of PLL in the film, the film prepared with PLL-FITC was removed from the glass substrate by the addition of 200 µl of 0.1 M NaOH, followed by 5 min of incubation in this solution. The film was lifted gently with the help of a forceps and resuspended in the solution gently to ensure total destruction (from both sides of the film). This treatment allows for complete removal of the multilayer film by deprotonation of PLL molecules. Then,

1.8 ml of 0.4 M Tris (containing 0.4 M NaCl, pH - 8.0) was added, and the fluorescence intensity was measured with a spectrofluorometer. The excitation wavelength was set at 490 nm, and the emission was measured at 520 nm with a slit value of 2 nm. The amount of PLL in the film was measured *via* a calibration curve using PLL-FITC solution.

### 2.3. Cell experiments

Mouse fibroblasts (subcutaneous) L929 (ACC 2), mouse fibroblasts (embryo) 3T3 (ACC 173), human embryonic kidney HEK-293 (ACC 305) and Chinese hamster ovary CHO-K1 were purchased from DSMZ, Germany. The human bone cell line U-2-OS was from Marinpharm GmbH, Germany and human primary fibroblasts from human fore skin were obtained from Charite hospital, Berlin, Germany. Dulbecco's modified Eagles' medium (Hepes modification) and fibronectin were from Sigma-Aldrich, Germany. Ham's F12 (with stable glutamine), foetal calf serum, L-alanyl-L-glutamine, phosphate buffered saline, trypsin-EDTA solution, trypan blue, penicillin-streptomycin and gentamycin were from Biochrom AG, Germany. The cell proliferation reagent WST-1 was from Roche diagnostics, Germany. The CELLSTAR 24 well cell culture multiwall plates were from Greiner Bio-one, Germany and the Nunc HydroCell Surface 24 well multidishes were from Nunc GmbH, Germany. The cell images were taken using a DM IL inverted phase contrast microscope, Leica Microsystems, Germany, and live cell monitoring was done in the Cell<sup>R</sup> platform of the IX 81 inverted fluorescence microscope with a MT-20 illumination system from Olympus Deutschland, Germany.

#### 2.3.1. Culture conditions

The cells were cultured as detailed in **Table 1**.

Table 1

The cell seeding was done at a density of  $10^5$  cells in  $25\text{ cm}^2$  T-flasks and  $10^4$  cells on the coverslips. The cells were maintained at  $37^\circ\text{C}$  in an incubator with 5%  $\text{CO}_2$  and observed periodically for their response. Sub-culturing of the flasks was carried out when the cells formed around 70-80% of a monolayer. Unless mentioned differently, usual analysis of cells on films was done 3 days after the cell seeding, which allows enough time for adhesion, spreading and proliferation on the surface.

### 2.3.2. Cell spreading

The cells were monitored for their adhesion and spreading by microscopic analysis. The phase-contrast images of the cells on the films were captured 3 days after cell seeding. The images were treated using Cell<sup>^</sup>R software, and the total number of spread cells in various microscopic fields was counted to deduce the spreading percentage. The total area occupied by the cells on the surface was also calculated using the software options. In the same manner, the size of the round cells was also calculated by measuring the cell diameter.

### 2.3.3. Live cell imaging

For live cell imaging experiments, the ‘experiment manager’ tool of the Cell<sup>^</sup>R software was exploited to make automated snapshots during defined intervals, namely every half-hour in this case. The various options of Cell<sup>^</sup>R such as automated stage movement combined with time-lapse and autofocus enable live cell data acquisition. The seeding of cells in a climate chamber with controlled gas and temperature conditions ensures precise monitoring of the cell response from the point of seeding until the end.

### 2.3.4. Cell viability - Trypan blue test

The viability of the cells was assessed by the trypan blue exclusion test on monolayer cells. Trypan blue (0.5%, w/v) diluted with PBS (1:1) was used for the test. The medium was carefully removed from the cells on the film and gently washed twice with PBS. The buffer was discarded, 300  $\mu\text{l}$  of trypan blue was added to cover the monolayer and incubated for about 8

min. Then, the residual dye was removed by PBS wash. The sample was observed under a microscope for dead cells that stained blue.

#### 2.3.5. Cell proliferation

WST assay according to the manufacturer's protocol.

#### 2.3.6. Fibronectin coating

Differing fibronectin concentrations (1  $\mu\text{g/ml}$ , 10  $\mu\text{g/ml}$  and 100  $\mu\text{g/ml}$ , diluted in millipore water) were used to coat the films and to incubate at 37°C for 1 h. Simultaneously, a control uncoated glass coverslip was also coated with 10  $\mu\text{g/ml}$  fibronectin. After incubation, the surfaces were rinsed with Millipore water and subjected to cell seeding. Images were recorded after 30 min, 1 h, and then onwards every 12 h.

#### 2.3.7. Counting of embryoid bodies

The mESCs were maintained in Petriplates before their seeding on surfaces. The Petri plates were covered with 0.1% gelatin overnight before seeding. The gelatin was removed and medium was added to the petriplate during cell seeding. To estimate the number of embryoid bodies on different surfaces, the cell medium containing these bodies on the films was taken and sedimented in a 15 ml Falcon tube by centrifuging at 800 rpm for 5 min. The supernatant was carefully removed and the embryoid bodies were suspended again carefully in 2 ml of fresh medium. The medium containing embryoid bodies was transferred to an ibidi  $\mu$ -dish and the number of embryoid bodies (which would be distinctly visible as huge cell clumps) was counted using microscopy.

### **3. Results and Discussion**

#### **3.1. Response of L929 cells to HA/PLL film**

Of the several methods available for LbL build-up like dip coating, spin coating, spraying, etc., the most commonly used one to date is dip coating<sup>[37]</sup> due to its efficiency, economy, speed and reliability. Hence, dipping was chosen as the suitable method to deposit

HA/PLL films in this study. The (HA/PLL)<sub>n</sub> films have been fabricated, with 'n' referring to the number of bilayers, where one bilayer corresponds to one complete deposition step, indicating the combined steps of complete polyanionic (HA) and polycationic (PLL) immersion events, together with the intermittent rinses. Further, to show the film sequence we will indicate either the 'n' number or the number of bilayers (bL). All the (HA/PLL)<sub>n</sub> films have been terminated with PLL. The prepared films were used directly for cell seeding after a thorough gentle rinse with Millipore water in order to remove excess of unbound salts from the surface.

In this study, the interaction of different types of cells with HA/PLL films was tested in terms of their adhesive, spreading and proliferative behaviour. Firstly we have focused on the response of one cell type (L929 fibroblasts cells), and the establishment of a correlation between the film properties and cellular behaviour. **Figure 1** summarizes the morphologies and distributions of L929 cells, attached to the films 3 days after their seeding. L929 cells exhibited clearly distinct morphologies with varying bL numbers. In case of 3 and 6 bL, the cells reached confluence in 3 days, similar to that of the control glass surface without any film coating. The cells did spread on films with 9 and 12 bL, but to a lesser extent in the case of 3 bL. For 15 bL, cell spreading was still less (also with some round unattached cells). However, in case of 18 and 24 bL, the cells did not show any attachment at all; rather, they formed clumps and floated over the surface, as also in the case of cells grown over commercial anti-adhesive surfaces (Fig. 1i).

Fig. 1.

Some other morphological features that could be recorded for L929 cells run are: These cells show a spreading of  $30 \pm 5$  % on films with 12 bL, and the spread cells occupy an area of  $655 \pm 182 \mu\text{m}^2$ . In case of the unspread round cells, they form clumps (resulting from cell-cell aggregation), whose features also differ between films with 12 and 24 bL. On the films with 12

bL, L929 cells rarely form clumps; when they do, the clumps are larger ( $138 \pm 29 \mu\text{m}$ , in diameter) and fewer in number, whereas on the 24 bL films, these clumps are relatively smaller ( $66 \pm 11 \mu\text{m}$ , in diameter, less than almost half compared to those on 12 bL) and higher in number. However, the size of the unspread, attached round cells on 12 and 24 bL do not differ. On 12 bL these cells are  $17 \pm 2 \mu\text{m}$  in size, and on 24 bL the average size was  $15 \pm 2 \mu\text{m}$ . A change in the terminating layer (HA instead of PLL) does not alter the adhesive response of the cells on 12 and 24 bL, thus indicating that certain bulk features of the films play a dominant role for cell adhesion rather than surface chemistry of the films.<sup>[38]</sup>

Next to cell adhesion as a response to a surface, it is essential to mark a difference in the proliferative capacity of the cells. Along these lines, the proliferation of cells on the films was tested, and the results of a cell proliferation assay are shown in **Figure 2a** (bL number vs. cell number). As can be seen from the graph, the proliferation of L929 cells on 3 and 6 bL is comparable to that of the control uncoated glass, while from 9 bL the proliferation starts decreasing (almost about 50 % of the control). On 12 bL the proliferation is around 35 % of that of the control, while from 15 bL the values reach less than 20 %. The reduction of proliferation of the cells can be attributed to a retarded metabolism of the cells when they are on a unfavourable surface.<sup>[33]</sup>

Fig. 2b gives an idea about the difference in the extent of metabolism by HEK-293 cells over 12 and 24 bL, indicating that the cells are metabolically active over 12 bL and not over 24 bL. The cells on HA/PLL films (on both 12 and 24 bL) respond to a cell viability test based on trypan blue, showing that the films are non-cytotoxic (data not shown). Several reports about cell-surface interactions indicate that the stiffness of the matrix upon which cells grow could have large effects on the structure (morphology and internal organisation) and function (proliferation, migration, etc.) of cells.<sup>[3, 39-41]</sup>

Fig. 2.

### 3.2. Film growth, morphology and softness

Here, we focus on the correlation between physico-chemical properties of HA/PLL films and cellular response. To minimize an effect of chemical cue on the cellular response, we have kept the chemical composition of the films similar (the last layer always being PLL). The HA/PLL films may differ not only in their mechanical properties as a function of deposited layers but also in their morphological/topological characteristics that may affect cellular response. Thus, mechanical and topological cues of the PEM films should be considered during the study of cellular response. In this context, mechanical and morphological features of the HA/PLL films are correlated with cellular response (adhesion) as a function of layer number.

The stiffness of (HA/PLL)<sub>n</sub> films with varying bL number is summarized in **Figure 3a**. To quantify the mechanical properties of bL of different numbers ‘n’, the elastic modulus of the films was measured by colloidal probe force spectroscopy.<sup>[42]</sup> As expected, smaller elastic moduli were obtained as bL number increased. This indicates that the film becomes softer with increasing bL number. Until 15 bL, the values of the Young’s modulus are in the range of 100-200 kPa and just above 15 bL, the modulus is reduced significantly up to one order of magnitude (for 30 bL). The HA/PLL films also vary in their morphology with differing bilayer numbers, as could be evidenced from Fig. 3b. It can also be inferred from the film morphology studies that the inhomogeneities might be a reason for the high standard deviations in the Young’s modulus measured for the films below 12 bL (Fig. 3a).

Fig. 3.

Overall, the variation of the mechanical properties correlates with changes in cell adhesion and proliferation, i.e., on relatively soft surfaces (> 15 bL) the cells show very little or no adhesion, while on stiffer surfaces ( $\leq$  15 bL), the cells exhibit reasonable adhesive and

proliferative characteristics (Fig. 1 and 2a). The threshold corresponds to the Young's modulus of 100 kPa (15 bL). Fibroblasts' repulsion to soft films is a well-established phenomenon, and a number of studies already showing that fibroblasts tend to adhere on surfaces with increased rigidity strongly support these findings.<sup>[3, 43]</sup> As a control, the adhesion of 3T3 and L929 fibroblasts over 12 and 24 bL of PSS/PAH films was tested (Supplementary Information, Fig. S1). The PSS/PAH films are known to be a linearly growing system with low polymer hydration and thus are much stiffer than HA/PLL ones. The terminating layer (PAH or PLL) brings to these films similar chemical composition of the film surface because both polycations have a primary aminogroup. Thus, the PSS/PAH film may be considered as a reference system which differs by softness.<sup>[44]</sup> In the case of PSS/PAH films, the cells adhere and spread well over both 12 and 24 bL, suggesting that softness plays an important role in determining the adhesion of cells on surfaces. The results agree with the widely accepted concept in the field of mechanobiology that living cells change their structure and functions as a response to surface softness<sup>[1, 45]</sup>, and that a variety of physiological processes occurring in the cell is influenced by the mechanical stress exerted at cell-substrate and cell-cell interfaces.<sup>[46]</sup>

One could assume that an increase of film softness with increase of the bL number might be associated with differing water content in the film. In other words, the polymer density in the film might vary depending on the layer number. However, it has been recently shown that softness of the HA/PLL film as measured by colloidal probe force spectroscopy and nanoindentation is not changed in the range of bilayer number from 12 to 96.<sup>[47]</sup> In order to prove this, we have compared film thickness and polymer (PLL) content in the film at different bL number (Fig. 3c, 3d). A linear correlation is established between the thickness of the dried films and the PLL content in the wet films (the slopes for the linear part of the growth profiles are the same). By assuming that the dried films lose water molecules independent of the bL number, the linear correlation would imply that the films possess the same polymer density. Thus, taking into account the conclusions above, the cell behavior noticed can be clearly

attributed to the film mechanical properties. We exclude that leaching of PLL from the film (PLL is mobile polymer) does affect cellular response because for cellular studies the films were exposed to cell culture medium for a long time.

### 3.3. Response of various cell types

The next obvious question that would arise is, whether this kind of behavior of cells (mechanics-dependent adhesive and spreading properties) on HA/PLL films is restricted only to L929 fibroblasts, or if it also applies to other cell types. To answer this, different types of cells were tested on (HA/PLL)<sub>n</sub> for their spreading. They include: mouse NIH-3T3 fibroblasts, human foreskin primary fibroblasts VH-Fib, human embryonic kidney HEK-293, human bone cell line U-2-OS and Chinese hamster ovary CHO-K. The cells were tested on the HA/PLL films with 12 and 24 bL, as from the results with L929 cells it became clear, that these two films show extreme spreading properties (cell adhesive and repellent, respectively). All these cell lines show good spreading over 12 bL, but over 24 bL, their spreading response is very poor, or almost none (**Figures 4, 5**). Thus, the changes in mechanical properties of HA/PLL films (from 12 bL and 24 bL, for instance) induce similar adhesive and spreading response for the diverse cell types.

Fig. 4.

Fig. 5.

Along the aspects mentioned above, it would be interesting to check if cell types like stem cells also show some difference in their response when cultivated on 12 and 24 bL films. Stem cells are more demanding in respect to the cultivation conditions in comparison to standard cell lines, and hence respond highly sensitive when testing any material for biomedical applications. In this regard, the adhesion and growth of the mES cell line E14 was tested on (HA/PLL)<sub>n</sub> films. The results obtained by the cell seeding experiments are summarized in

**Figure 6.** After 36 h, the cells on 12 bL formed small clumps (Fig. 6a), resulting from the aggregation of individual cells. These clumps grow in size over time. After 5 days, they become big clumps reaching diameters even bigger than 100  $\mu\text{m}$  (Fig. 6g). On 24 bL, the cells remain attached as individual entities (Fig. 6b), and also over time remain independent, or at the most, form only very small clumps (Fig. 6h). On a control glass coverslip with no film coating, these non-differentiated cells formed well-defined colonies of characteristic shape and a partial 3-D structure (Fig. 6i). Similar morphological observations were reported for mES cell line D3 cultivated over surfaces containing PEI or PLL with some extracellular matrix (ECM) proteins.<sup>[48]</sup>

Fig. 6.

The cell clumps of varied size correspond to the embryoid bodies that most probably result from cell-cell interaction in stem cell colonies.<sup>[49]</sup> Such embryoid bodies are usually formed by stem cells as three-dimensional structures,<sup>[50]</sup> when the intercellular interactions (be it direct contacts between cells or indirect via the ECM) play a dominant role. The role of these embryoid bodies in *in vivo* systems is noticeable as precursors, from which spontaneous differentiation of stem cells into a large variety of cell types occurs.<sup>[51]</sup> The size and attachment properties of such embryoid bodies formed over 12 and 24 bL films also differ from each other. For example, on 12 bL, large, few (in number) clumps are noticed, whereas over 24 bL, these clumps are small, more in number and remain partially attached to the surface. The size of the embryoid bodies on 12 bL ( $138 \pm 29 \mu\text{m}$ ) was almost double as those on 24 bL ( $67 \pm 11 \mu\text{m}$ ).

Yet another noticeable aspect here is the difference in morphology of the cells in the uncoated regions outside the 12 and 24 bL films. This effect is illustrated in **Figure 7**. The cells outside the 12 bL spread well on glass; the spreading increases over time and after 5 days, they resemble almost those grown on the control surfaces without any film in the vicinity (Fig. 6i and Fig. 7). On the other hand on 24 bL films even these cells outside the film on glass are not

able to spread well and they form embryoid bodies, just as in the case of cells grown on the 12 bL films. This effect could be attributed to certain biochemical signalling occurring between the cells grown on the film and on the glass in the vicinity of the film. Thus, the role of soluble factors in cell-PEM interaction is seen to modulate the growth and spreading of the neighbouring cells as well.

Fig. 7.

### **3.4. Effect of Fibronectin coating**

Another interesting feature to be noted from the adhesion and spreading behavior of different types of cells to HA/PLL films is that the response does not depend on treatment procedures affecting surface properties like terminating deposition step or pre-treatment (related to the rinsing protocols used to clean the surfaces before film deposition) (Supplementary Information, Fig. S2). In this context, it becomes interesting to notice, if some ECM proteins like fibronectin could bring about a change in the adhesive and spreading behavior of cells grown on these surfaces.

Fibronectin is not able to bring about any change in the behaviour of cells on soft films (Supplementary Information, Fig. S3). Even a high concentration of a cell-adhesive protein like fibronectin (100 µg/ml in solution, used to coat 1 cm<sup>2</sup> of the surface), about 10 times higher than that normally used for coating a cell culture dish) does change the spreading behaviour of cells. We expect that fibronectin is adsorbed on the film surface, because many of the model proteins, independent of their charge and size, have high affinity to the HA/PLL film.<sup>[35]</sup>

On 12 bL, it can be seen that both 3T3 and L929 cells, with (Fig. S3 a and e, respectively) and without fibronectin (Fig. S3 b and f, respectively) spread more or less to the same extent. On 24 bL films also fibronectin does not lead to any drastic change in the spreading of 3T3 and L929 cells (Fig. S3 c and d, and g and h, respectively), in the sense that the cells remain spherical either singles (as in 3T3) or in clumps (as in L929).

The results indicate that cell adhesion and spreading on HA/PLL films can be independent of fibronectin binding to the film surfaces. In other words, HA/PLL films influence cell behaviour in a manner independent of ECM protein interaction, and this highlights the dominance of substrate mechanics in cellular response. However, the probable unfolding of fibronectin molecules<sup>[52]</sup> due to their interaction with the polyelectrolytes in the presence of salt stored in the film or polyelectrolytes as film constituents is not to be excluded. The resulting cellular response is to be considered as an outcome of the interplay between the mechanics and biochemistry of the cellular microenvironment. It should also be mentioned that there are currently no data available on biochemical pathways leading to such cellular responses on soft films, which stimulates further work in these directions.

### 3.5. 'Cell-friendly window'

From the response of diverse cell types to the HA/PLL films, we propose a narrow 'cell-friendly' window for this PEM system, as represented in **Figure 8**. The window is between 12 and 15 bL for HA/PLL films for favourable cell spreading under the experimental conditions chosen (Fig. 8, green-coloured region). For all cell types tested, the adhesive and spreading behaviour of the cells does not depend on post-treatment of the substrate with fibronectin as a representative protein for promoting cell adhesion. Also, other manipulations like pre-treatment of surfaces for film deposition (Supplementary Information, Fig. S2) and presence of serum in cell culture medium (Supplementary Information, Fig. S4) did not alter this window. Below this window region (Fig. 10, yellow-coloured region), the films get deposited as islands, and are not homogeneous (Fig. 3b). Hence, despite the good cell adhesive nature of this region, the HA/PLL film with  $n < 12$  cannot be considered as suitable films for bio-applications. Likewise, above this window (Fig. 10, orange-coloured region), the HA/PLL films are homogeneous in morphology, but they do not support cell adhesion (Fig. 1, 4 and 5). However, this region is very attractive due to its reservoir capacity and hence, it shall be certainly useful for loading

and delivery of desired biomolecules. It is obvious that the higher the bL number, the thicker the film is, and hence, the higher the capacity to embed molecules in its interior.<sup>[53, 54]</sup>

Fig. 8.

### 3.6. Future perspectives

The extension of the identified ‘cell-friendly’ window is desirable to exploit the high reservoir capacity of the PEM films to be used for biologically relevant applications. In other works from our group, we have shown ways to extend this ‘cell-friendly’ window by varied approaches, namely mechanical reinforcement of films<sup>[36, 55]</sup> or microfluidic-assisted 3D cell patterning.<sup>[42]</sup> It seems that improvement of cellular adhesion by changing the chemical composition on the surface of soft HA/PLL films (e.g. adsorption of additional layer of cell-adhesive polymer) does not represent a rational approach to make the films cell-adhesive. Mechanical reinforcing or templating may be rather promising for this purpose.

When properly exploited, this extended ‘cell-friendly window’ can be used for targeted release (making use of the reservoir properties of the film) to locally deliver biomolecules to desired cells. Bioactive molecules can be loaded directly into the preformed PEMs (post-loading)<sup>[35]</sup> or trapped as constituents of the film during the LbL assembly process (embedding).<sup>[56-59]</sup> Another option is to load the PEM films with carriers encapsulating the biomolecules. These carriers might be polyelectrolyte microcapsules<sup>[60-62]</sup> or, in principle, protein microparticles, which can be formulated into a particular form at mild conditions.<sup>[63, 64]</sup> Additionally, the biomolecule-loaded films may be exploited for non-invasive release (e.g. light-triggered,<sup>[65, 66]</sup> since a number of stimuli-sensitive release methods have already been reported.<sup>[14, 67-69]</sup>

It has already been demonstrated that the developmental fate of the pluripotent stem cells is determined not only by soluble factors, but also by the ECM.<sup>[70]</sup> Thus, the HA/PLL films

could be conceived as a potential extracellular ‘niche’ for the growth of these cells (not only in terms of their reservoir capacities for growth factors and differentiation molecules, but also as a matrix to modulate the interaction *via* integrin and other cell adhesion molecules, that shall influence the expression of relevant signalling molecules needed for the metabolic regulation). In terms of differentiation, in addition to the ECM environment, the films might also determine the developmental pathway of the stem cells<sup>[71]</sup> by directing their differentiation in an autocrine or paracrine manner via enabling the secretion of humoral factors and other proteins. Moreover, the films could be possibly used to moderate efficient engagement of integrin receptors and other cell adhesion molecules, thus directing the differentiation process in a coordinated manner. Thus, new routes for directing the differentiation of stem cells into desired phenotypes are achievable using these PEM systems. The use of such films can also be extended to cancer cell lines to understand, for instance, metastasis development where substrate properties (that mimic the dynamic cellular microenvironment) may be crucial in establishing features related to pathological processes.

The physical and mechanical cues of the ECM are transduced into biochemical changes through complex mechanisms not yet fully understood, resulting in the response noticed, be it morphological or at signal transduction levels. The correlation shown between the film mechanical properties and cellular response is to be considered as a direct evidence of the feedback of local matrix stiffness to cellular response. The main issues to be resolved in modern mechanobiology concern the molecular details of the material that are actually sensed by the cell and whether the sensing mechanism of the cells is related to what is known from biological systems. This should come into consideration in future for understanding of the mechanobiological aspects of cell-PEM interaction.

Finally, it becomes evident that a systematic understanding of the PEM-cell interaction would go a long way in bridging the gap between material science and cell biology.

## **4. Conclusions**

In this study, we have defined a narrow ‘cell-friendly’ window for the HA/PLL film - between 12 and 15 bL. Within this window, all the various tested cells spread well. Outside this window, the films are either non-homogeneous (below 12 bL) or cell-repellent (above 15 bL). Cellular adhesion correlates with mechanical properties of the film. When increasing the bilayer number, the films become softer. The threshold for cellular adhesiveness (15 bL) corresponds to a Young’s modulus of about 100 kPa. Immersion of the film with the cell-adhesive protein fibronectin or addition of serum to the cell culture medium do not lead to changes of the cellular behaviour. This might indicate that mechanical cues provided by the films are highly relevant and cell growth is a result of an interplay of both biochemical and mechanical cues. Stem cells form embryoid bodies on the film surface. It has been found that for small bL numbers the embryoid bodies are larger in size and less in number compared to what has been observed on thicker films. The window becomes significant for driving PEM systems towards novel biomedical applications such as controlled release of biomolecules to adjacent cells.

## **Supporting Information**

Supporting Information is available from the Wiley Online Library or from the author

### **Acknowledgements:**

DV thanks the Alexander von Humboldt Foundation for support (AvH Fellowship and Sofja Kovalevskaja Program). The authors would like to thank Beate Morgenstern for assistance in cell culture experiments. NM acknowledges the funding from IMPRS on Biomimetic Systems (MPI-KG).

Received: Month XX, XXXX; Revised: Month XX, XXXX; Published online:

((For PPP, use “Accepted: Month XX, XXXX” instead of “Published online”)); DOI: 10.1002/marc.((insert number)) ((or ppap., mabi., macp., mame., mren., mats.))

**Keywords:** cell adhesion, layer-by-layer, softness, Young’s modulus, colloidal probe

## References

- [1] F. Rehfeldt, A. J. Engler, A. Eckhardt, F. Ahmed, D. E. Discher, *Adv Drug Deliv Rev* **2007**, *59*, 1329.
- [2] R. G. Flemming, C. J. Murphy, G. A. Abrams, S. L. Goodman, P. F. Nealey, *Biomaterials* **1999**, *20*, 573.
- [3] D. E. Discher, P. Janmey, Y. L. Wang, *Science* **2005**, *310*, 1139.
- [4] D. E. Ingber, *FASEB J* **2006**, *20*, 811.
- [5] D. E. Jaalouk, J. Lammerding, *Nat Rev Mol Cell Biol* **2009**, *10*, 63.
- [6] J. H. Kim, L. J. Dooling, A. R. Asthagiri, *J R Soc Interface* **2010**, *7 Suppl 3*, S341.
- [7] T. Mammoto, D. E. Ingber, *Development* **2010**, *137*, 1407.
- [8] M. Delcea, S. Schmidt, R. Palankar, P. A. Fernandes, A. Fery, H. Möhwald, A. G. Skirtach, *Small* **2010**, *6*, 2858.
- [9] Y. Lvov, G. Decher, H. Haas, H. Möhwald, A. Kalachev, *Physica B* **1994**, *198*, 89.
- [10] Y. Lvov, G. Decher, G. Sukhorukov, *Macromolecules* **1993**, *26*, 5396.
- [11] G. Decher, J. D. Hong, J. Schmitt, *Thin Solid Films* **1992**, *210*, 831.
- [12] G. Decher, *Science* **1997**, *277*, 1232.
- [13] D. Volodkin, A. Skirtach, H. Mohwald, *Bioactive Surfaces* **2011**, *240*, 135.
- [14] Z. Y. Tang, Y. Wang, P. Podsiadlo, N. A. Kotov, *Advanced Materials* **2006**, *18*, 3203.
- [15] S. Pavlukhina, S. Sukhishvili, *Advanced Drug Delivery Reviews* **2011**, *63*, 822.
- [16] T. Boudou, T. Crouzier, K. F. Ren, G. Blin, C. Picart, *Advanced Materials* **2010**, *22*, 441.

- [17] D. Volodkin, R. von Klitzing, *Current Opinion in Colloid & Interface Science* **2014**, *19*, 25.
- [18] R. von Klitzing, *Physical Chemistry Chemical Physics* **2006**, *8*, 5012.
- [19] J. B. Schlenoff, S. T. Dubas, *Macromolecules* **2001**, *34*, 592.
- [20] N. Madaboosi, K. Uhlig, M. S. Jaeger, H. Moehwald, C. Duschl, D. V. Volodkin, *Macromolecular Rapid Communications* **2012**, *33*, 1775.
- [21] H. Isaksson, *Mechanics Research Communications* **2012**, *42*, 22.
- [22] J. Liu, N. Sun, M. A. Bruce, J. C. Wu, M. J. Butte, *PLOS ONE* **2012**, *7*, e37559.
- [23] W. J. Tyler, *Nat Rev Neurosci* **2012**, *13*, 867.
- [24] Y. Sun, J. Fu, *Integrative biology : quantitative biosciences from nano to macro* **2013**, *5*, 450.
- [25] L. MacQueen, Y. Sun, C. A. Simmons, *Journal of The Royal Society Interface* **2013**, *10*.
- [26] N. Aggarwal, N. Altgarde, S. Svedhem, K. Zhang, S. Fischer, T. Groth, *Langmuir* **2013**, *29*, 13853.
- [27] N. Aggarwal, N. Altgarde, S. Svedhem, K. Zhang, S. Fischer, T. Groth, *Colloid Surf. B-Biointerfaces* **2014**, *116*, 93.
- [28] N. E. Muzzio, M. A. Pasquale, D. Gregurec, E. Diamanti, M. Kosutic, O. Azzaroni, S. E. Moya, *Macromol. Biosci.* **2016**, *16*, 482.
- [29] N. E. Muzzio, D. Gregurec, E. Diamanti, J. Irigoyen, M. A. Pasquale, O. Azzaroni, S. E. Moya, *Advanced Materials Interfaces* **2017**, *4*.
- [30] T. Crouzier, K. Ren, C. Nicolas, C. Roy, C. Picart, *Small* **2009**, *5*, 598.
- [31] K. Ren, L. Fourel, C. G. Rouvière, C. Albiges-Rizo, C. Picart, *Acta Biomaterialia* **2010**, *6*, 4238.
- [32] G. Blin, N. Lablack, M. Louis-Tisserand, C. Nicolas, C. Picart, M. Puceat, "Nano-scale control of cellular environment to drive embryonic stem cells selfrenewal and fate", 2009, p. 1742.

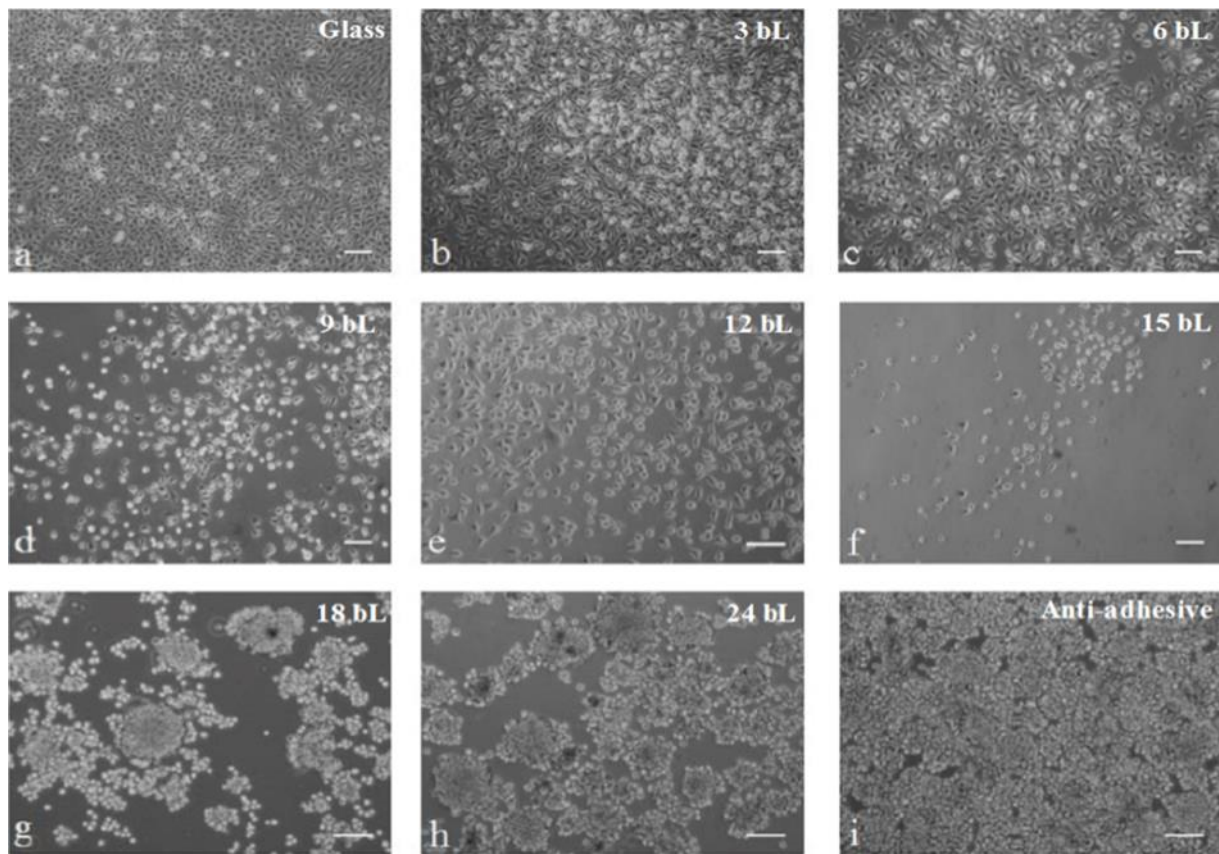
- [33] T. Boudou, T. Crouzier, C. Nicolas, K. Ren, C. Picart, *Macromolecular Bioscience* **2011**, *11*, 77.
- [34] R. Zahn, E. Thomasson, O. Guillaume-Gentil, J. Vörös, T. Zambelli, *Biomaterials* **2012**, *33*, 3421.
- [35] K. Uhlig, N. Madaboosi, S. Schmidt, M. S. Jaeger, J. Rose, C. Duschl, D. V. Volodkin, *Soft Matter* **2012**, *8*, 11786.
- [36] S. Schmidt, N. Madaboosi, K. Uhlig, D. Koehler, A. Skirtach, C. Duschl, H. Moehwald, D. V. Volodkin, *Langmuir* **2012**, *28*, 7249.
- [37] T. Boudou, T. Crouzier, K. Ren, G. Blin, C. Picart, *Advanced Materials* **2010**, *22*, 441.
- [38] J. Y. Wong, J. B. Leach, X. Q. Brown, *Surface Science* **2004**, *570*, 119.
- [39] C. A. Reinhart-King, M. Dembo, D. A. Hammer, *Biophysical Journal* **2008**, *95*, 6044.
- [40] P. A. Janmey, J. P. Winer, M. E. Murray, Q. Wen, *Cell Motility and the Cytoskeleton* **2009**, *66*, 597.
- [41] A. J. Engler, L. Richert, J. Wong, C. Picart, D. Discher, "Surface probe measurements of the elasticity of sectioned tissue, thin gels and polyelectrolyte multilayer films: Correlations between substrate stiffness and cell adhesion", 2004, p. 142.
- [42] N. Madaboosi, K. Uhlig, S. Schmidt, M. S. Jaeger, H. Moehwald, C. Duschl, D. V. Volodkin, *Lab on a Chip* **2012**, *12*, 1434.
- [43] C.-M. Lo, H.-B. Wang, M. Dembo, Y.-l. Wang, *Biophysical Journal* **2000**, *79*, 144.
- [44] W. Qi, Z. Xue, W. Yuan, H. Wang, *Journal of Materials Chemistry B* **2014**, *2*, 325.
- [45] M. Dembo, Y.-L. Wang, *Biophysical Journal*, *76*, 2307.
- [46] C. Üzüüm, J. Hellwig, N. Madaboosi, D. Volodkin, R. von Klitzing, *Beilstein Journal of Nanotechnology* **2012**, *3*, 778.
- [47] E. Brynda, J. Pacherník, M. Houska, Z. Pientka, P. Dvořák, *Langmuir* **2005**, *21*, 7877.
- [48] E. Y. L. Fok, P. W. Zandstra, *STEM CELLS* **2005**, *23*, 1333.

- [49] J. Mittmann, I. Kerkis, C. Kawashima, M. Sukoyan, E. Santos, A. Kerkis, *Genetics and Molecular Biology* **2002**, *25*, 103.
- [50] A. G. Smith, *Journal of tissue culture methods* **1991**, *13*, 89.
- [51] G. Baneyx, L. Baugh, V. Vogel, *Proceedings of the National Academy of Sciences* **2002**, *99*, 5139.
- [52] S. Mansouri, F. Winnik, M. Tabrizian, "Modulating the release kinetics through the control of the permeability of the layer-by-layer assembly: A review", 2009, p. 585.
- [53] F. Meyer, M. Dimitrova, J. Jedrzejenska, Y. Arntz, P. Schaaf, B. Frisch, J.-C. Voegel, J. Ogier, *Biomaterials* **2008**, *29*, 618.
- [54] D. Kohler, N. Madaboosi, M. Delcea, S. Schmidt, B. G. De Geest, D. V. Volodkin, H. Moehwald, A. G. Skirtach, *Advanced Materials* **2012**, *24*, 1095.
- [55] N. Jessel, F. Atalar, P. Lavallo, J. Mutterer, G. Decher, P. Schaaf, J. C. Voegel, J. Ogier, *Advanced Materials* **2003**, *15*, 692.
- [56] D. V. Volodkin, N. G. Balabushevitch, G. B. Sukhorukov, N. I. Larionova, *Biochemistry-Moscow* **2003**, *68*, 236.
- [57] Y. Lvov, K. Ariga, I. Ichinose, T. Kunitake, *Journal of the American Chemical Society* **1995**, *117*, 6117.
- [58] N. G. Balabushevich, M. A. Pechenkin, E. D. Shibanova, D. V. Volodkin, E. V. Mikhailchik, *Macromol. Biosci.* **2013**, *13*, 1379.
- [59] A. S. Sergeeva, D. A. Gorin, D. V. Volodkin, *BioNanoScience* **2014**, *4*, 1.
- [60] M. A. Pechenkin, H. Moehwald, D. V. Volodkin, *Soft Matter* **2012**, *8*, 8659.
- [61] D. V. Volodkin, N. Madaboosi, J. Blacklock, A. G. Skirtach, H. Moehwald, *Langmuir* **2009**, *25*, 14037.
- [62] S. Schmidt, M. Behra, K. Uhlig, N. Madaboosi, L. Hartmann, C. Duschl, D. Volodkin, *Advanced Functional Materials* **2013**, *23*, 116.
- [63] S. Schmidt, K. Uhlig, C. Duschl, D. Volodkin, *Acta Biomaterialia* **2014**, *10*, 1423.

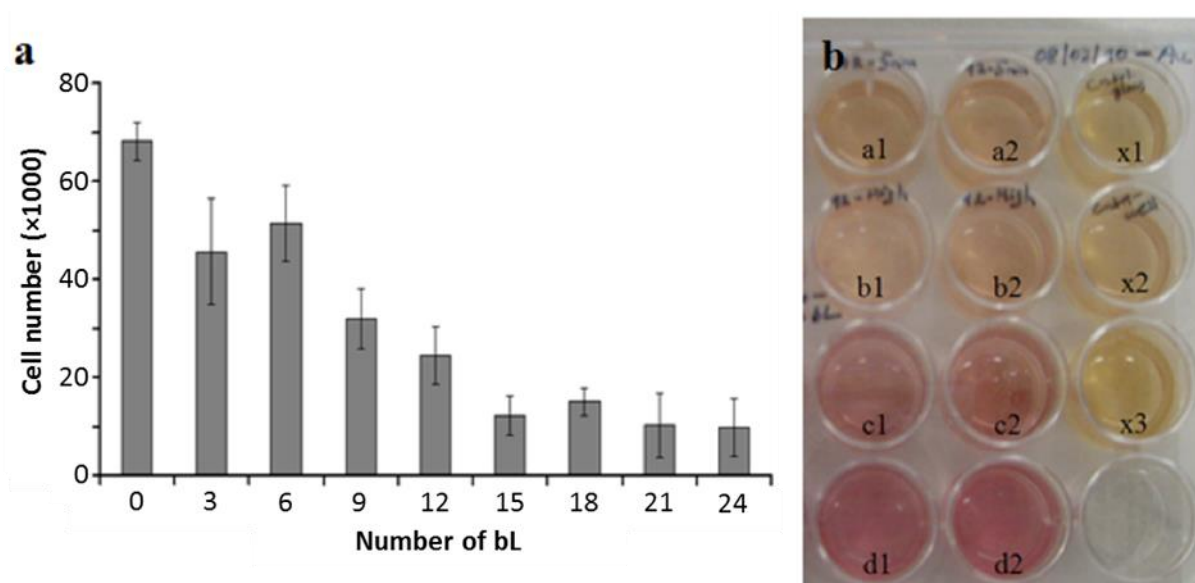
- [64] S. Schmidt, D. Volodkin, *Journal of Materials Chemistry B* **2013**, *1*, 1210.
- [65] D. Volodkin, A. Skirtach, N. Madaboosi, J. Blacklock, R. von Klitzing, A. Lankenau, C. Duschl, H. Mohwald, *Journal of Controlled Release* **2010**, *148*, E70.
- [66] S. A. Sukhishvili, *Current Opinion in Colloid & Interface Science* **2005**, *10*, 37.
- [67] E. Kharlampieva, V. Kozlovskaya, S. A. Sukhishvili, *Advanced Materials* **2009**, *21*, 3053.
- [68] P. Lavalle, J. C. Voegel, D. Vautier, B. Senger, P. Schaaf, V. Ball, *Advanced Materials* **2011**, *23*, 1191.
- [69] J. Czyz, A. M. Wobus, *Differentiation* **2001**, *68*, 167.
- [70] B. Trappmann, J. E. Gautrot, J. T. Connelly, D. G. T. Strange, Y. Li, M. L. Oyen, M. A. Cohen Stuart, H. Boehm, B. Li, V. Vogel, J. P. Spatz, F. M. Watt, W. T. S. Huck, *Nat Mater* **2012**, *11*, 642.
- [71] F. Chowdhury, S. Na, D. Li, Y.-C. Poh, T. S. Tanaka, F. Wang, N. Wang, *Nat Mater* **2010**, *9*, 82.

Table 1. Cell culture conditions for growth of various cell lines used in the study.

Cell Line	Medium used	Trypsin/ EDTA (w/v)	Trypsini- sation time (at 37°C)
L929	DMEM + 10% FCS + 4 mM L-alanyl-L-glutamine + 1% penicillin/streptomycin	0.05%, 0.02%	5 min
3T3	”	”	6 min
HEK-293	DMEM + 15% FCS + 4 mM stabilised L-glutamine + 1% pencillin/streptomycin	”	6 min
CHO-K1	Ham’s F-12 + 10 % FCS + 1% penicillin-streptomycin	0.25%, 0.02%	5 min
U-2-OS	DMEM + 10 % FCS + 4 mM L-alanyl-L-glutamine + 1% non-essential amino acids + 1% penicillin-streptomycin	”	6 min
E14	DMEM (knock-out) + 10% FCS + 2 mM L-glutamine + 1% non-essential amino acids + 1% gentamycin + 1000 Units/ml ESGRO-LIF	”	5 min
VH-Fib	as for L929	0.05%, 0.02%	6 min



*Figure 1.* Phase contrast images of L929 cells observed 3 days after seeding ( $1 \times 10^4$  cells/cm<sup>2</sup>) on (HA/PLL)<sub>n</sub> bilayers. a – cells on uncoated glass coverslip; b – on 3bL; c – on 6bL; d – on 9bL; e – on 12bL; f – on 15bL; g – on 18bL; h – on 24bL; i – on anti-adhesive surfaces from Nunc. Scale – 100  $\mu$ m.



**Figure 2. a.** Cell proliferation assay using the WST method. The total number of L929 cells on the (HA/PLL)<sub>n</sub> films is shown for varying bilayer numbers. 0 refers to a control uncoated glass coverslip with no film. **b.** The picture shows cell culture wells with cell culture medium metabolized by HEK-293 cells grown over (HA/PLL)<sub>n</sub> films; a1, a2 – color of the medium metabolized by cells seeded at a low density of ( $5 \times 10^3$  cells/cm<sup>2</sup>) grown on 12bL; b1, b2 – color of the medium metabolized by cells seeded at a high density of ( $2 \times 10^4$  cells/cm<sup>2</sup>) grown on 12bL; c1, c2 – color of the medium metabolized by cells seeded at a low density of ( $5 \times 10^3$  cells/cm<sup>2</sup>) grown on 24bL; d1, d2 – color of the medium metabolized by cells seeded at a high density of ( $2 \times 10^4$  cells/cm<sup>2</sup>) grown on 24bL; x1, x2 – controls of cells grown on an uncoated glass coverslip at a density of ( $5 \times 10^3$  cells/cm<sup>2</sup>) and x3 - control of cells grown on uncoated glass coverslip at a high density of ( $1 \times 10^4$  cells/cm<sup>2</sup>). The original medium contains phenol red, an pH-indicator, whose color changes from pink-purple (as in d1 or d2) to pale yellow (as in x1 and x2 or x3) as the cells in these wells metabolize the medium.

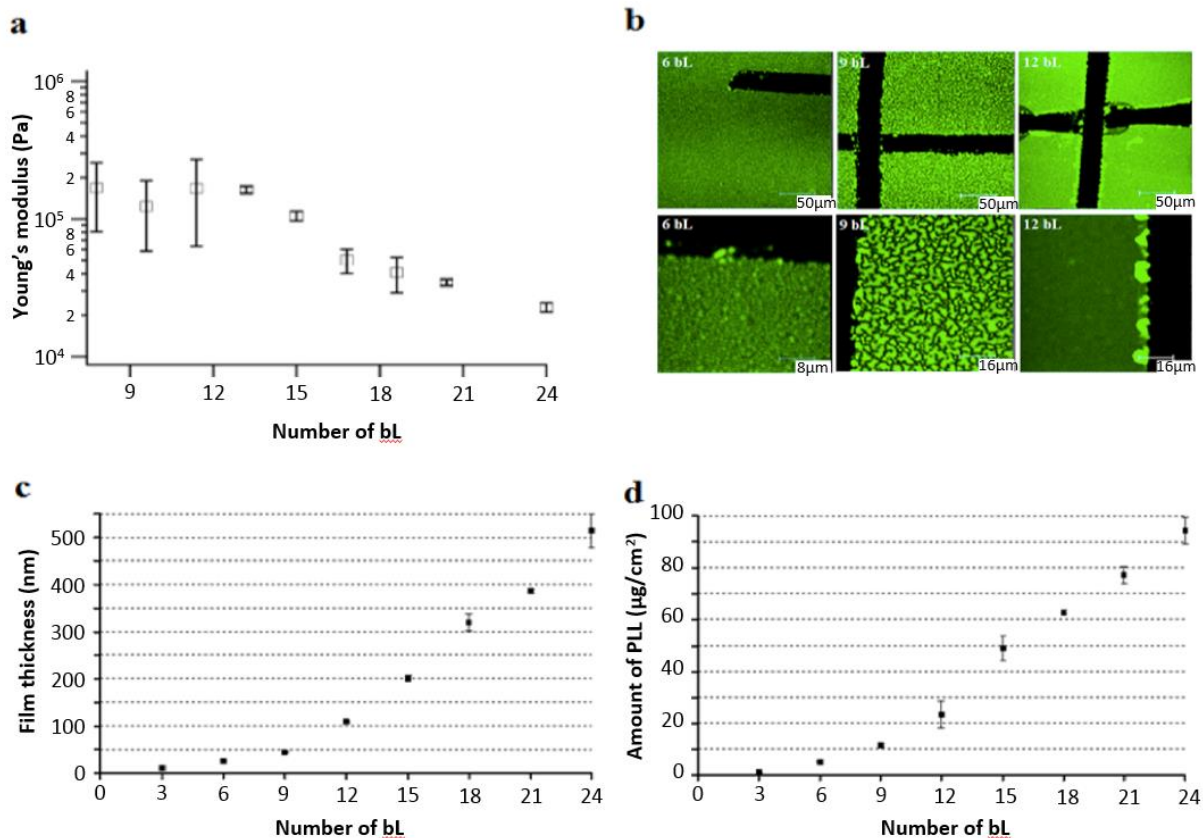


*Figure 3. a.* Young's modulus of different bL HA/PLL films. It can be seen that with increasing bL number, the films become considerably softer. *b.* CLSM images showing the morphology of the (PLL-FITC/HA)<sub>n</sub> films with n = 6, 9 and 12. It can be noticed that the film begins to grow in islands, which later coalesce to form a homogeneous film with the 12<sup>th</sup> bL. The images in the bottom row show magnified regions from the respective images in the top row. The black areas represent scratches where film is removed. *c.* Graph showing thickness measurements obtained from dry (HA/PLL)<sub>n</sub> films using AFM. *d.* Graph showing the amount of PLL present in (HA/PLL)<sub>n</sub>. The error bars represent the standard deviation among samples used.

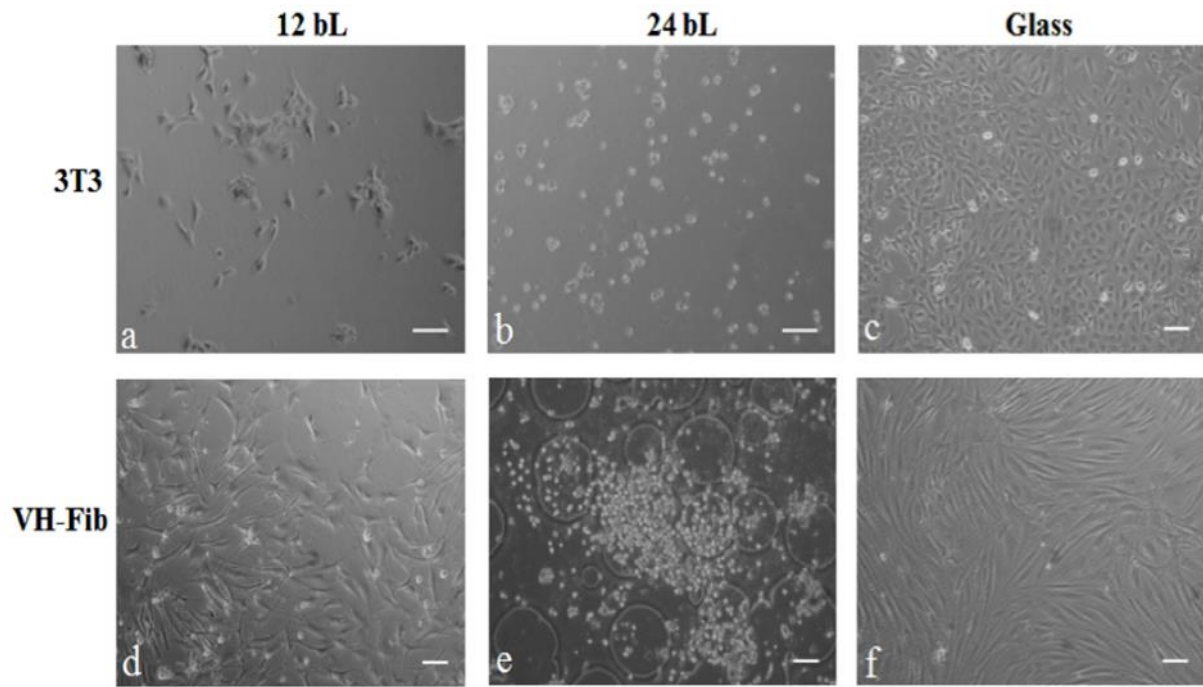


*Figure 4.* Phase contrast images of fibroblast cells observed after 3 days of seeding ( $1 \times 10^4$  per  $\text{cm}^2$ ) on  $(\text{HA}/\text{PLL})_n$  bilayers. a – 3T3 on 12bL; b – 3T3 on 24bL; c – 3T3 on an uncoated glass coverslip; d – Human foreskin primary fibroblast cells (VH-Fib) on 12bL; e – VH-Fib on 24bL; f – VH-Fib on an uncoated glass coverslip. Scale – 100  $\mu\text{m}$ .

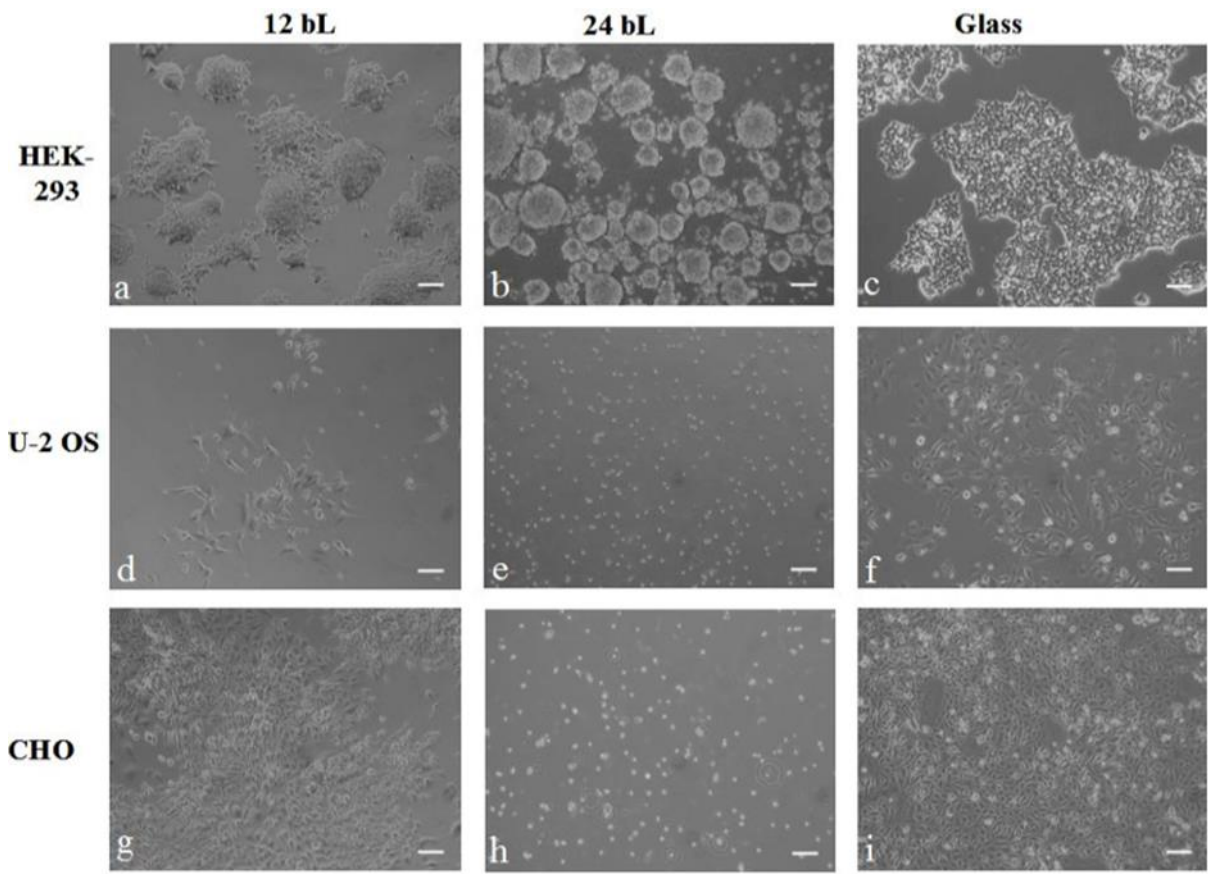


*Figure 5.* Phase contrast images of various epithelial cells observed 3 days after seeding ( $1 \times 10^4$  per  $\text{cm}^2$ ) on (HA/PLL) $_n$  bilayers. a – HEK-293 on 12bL; b – HEK-293 on 24bL; c – HEK-293 on an uncoated glass coverslip; d – U-2 OS on 12bL; e – U-2 OS on 24bL; f – U-2 OS on uncoated glass coverslip; g – CHO on 12bL; h – CHO on 24bL; i – CHO on an uncoated coverslip Scale – 100  $\mu\text{m}$ .

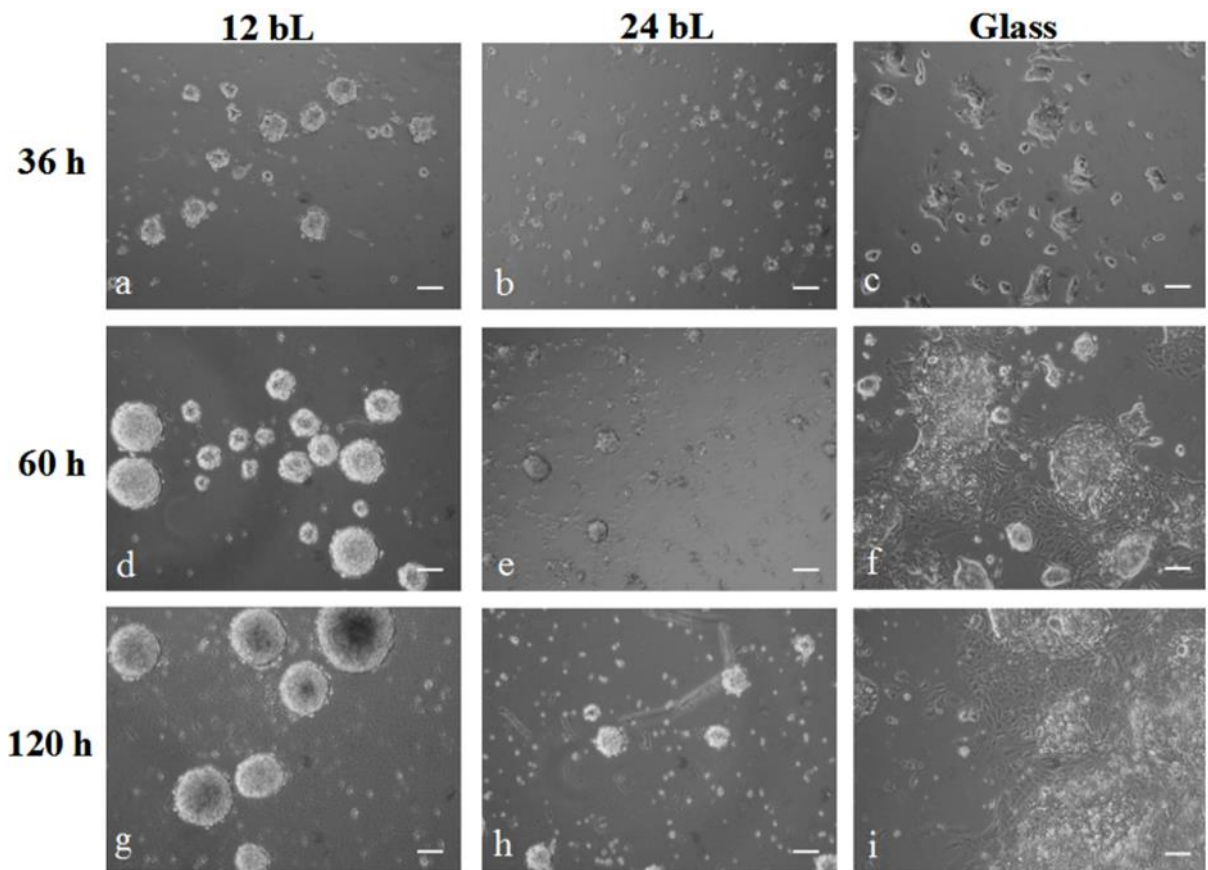


*Figure 6.* E14Tg2A mouse embryonic stem cells on (HA/PLL)<sub>n</sub> films – cells seeded at a density of  $5 \times 10^4$  per  $\text{cm}^2$ ; cultivation media with LIF were used to prevent differentiation. a - cells on 12 bL after 36 h; b - on 24 bL after 36 h; c - on an uncoated glass coverslip after 36 h; d - on 12 bL after 60 h; e - on 24 bL after 60 h; f - on an uncoated glass coverslip after 60 h; g - on 12 bL after 120 h; h - on 24 bL after 120 h; i - on an uncoated glass coverslip after 120 h. Scale – 100  $\mu\text{m}$ .

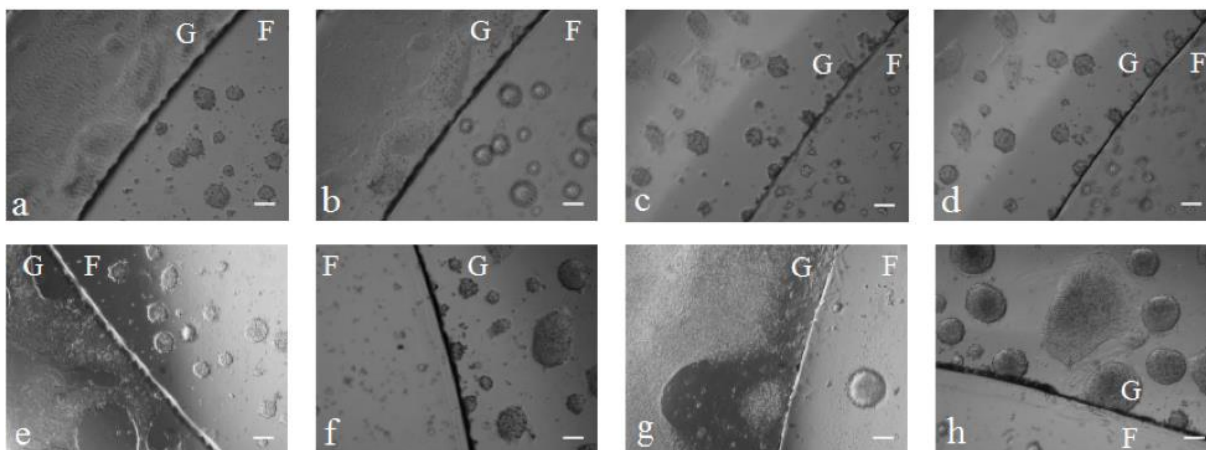


*Figure 7.* Morphology of E14 mES cells on uncoated glass in immediate vicinity of t12 and 24 bL HA/PLL films. ‘F’ represents the region where the cells are grown on the film surface and ‘G’ represents the region where cells are grown on uncoated glass, the boundary between the two regions being distinctly visible in all cases. a - cells on 12 bL after 36 h (focus on F); b - cells on 12 bL after 36 h (focus on G); c - cells on 24 bL after 36 h (focus on F); d - cells on 24 bL after 36 h (focus on G); e - cells on 12 bL after 60 h (focus on G); f - cells on 24 bL after 60 h (focus on G); g - cells on 12 bL after 120 h (focus on G); h - cells on 24 bL after 120 h (focus on G). Scale – 100  $\mu$ m.

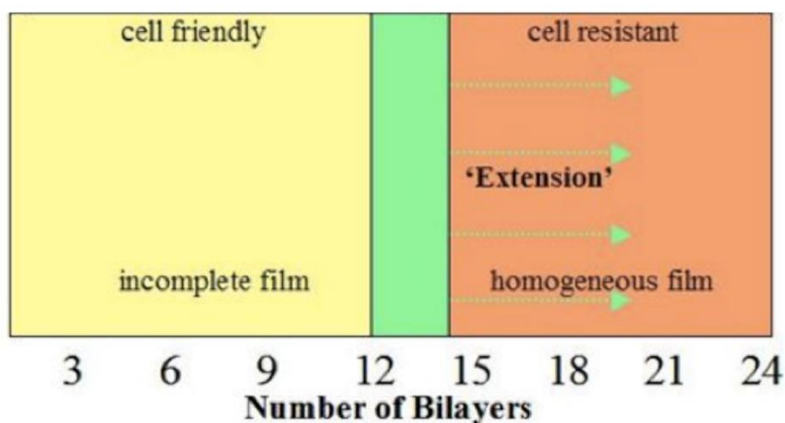


*Figure 8.* A ‘Cell-friendly window’ with a narrow range of numbers of bilayers has been postulated striking the balance between homogeneity of the HA/PLL film and conducive conditions for cell adhesion (shown in green). The yellow region shows good cell adhesion, but the films formed are inhomogeneous here; the orange region corresponds to a homogeneous film, but is cell-resistant. Green arrows represent the direction of the desired extension of the cell-friendly window.

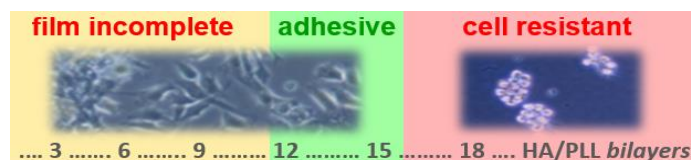
**A narrow “cell-friendly” window** (between 12 and 15 bilayers) is identified for cellular adhesion and growth onto biopolymer-based hyaluronic acid/poly-L-lysine multilayers. Cellular response including formation of stem cell embryoid bodies is governed by the softness of the multilayers, which in turn correlates with the bilayer number. Extending this window is vital for driving multilayers towards modern cell-based bio-applications.

Narayanan Madaboosi,<sup>a,b</sup> Katja Uhlig,<sup>a</sup> Stephan Schmidt,<sup>a,c</sup> Anna S. Vikulina,<sup>d</sup> Helmuth Möhwald,<sup>b</sup> Claus Duschl,<sup>a</sup> Dmitry V. Volodkin<sup>a,d\*</sup>

Corresponding author: Dr Dmitry V. Volodkin,  
Email: [dmitry.volodkin@ntu.ac.uk](mailto:dmitry.volodkin@ntu.ac.uk)

### **A “cell-friendly” window for the interaction of cells with hyaluronic acid/poly-L-lysine multilayers**

ToC figure



## Supporting Information

for *Macromol. Biosci.*, DOI: 10.1002/mabi.2013#####

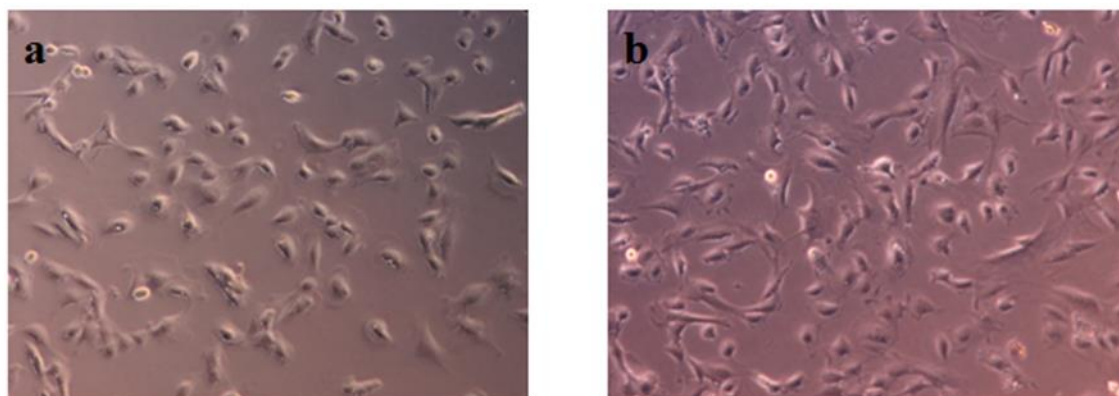


**Fig. S1.** Phase contrast images of 3T3 cells observed 2 days after seeding ( $1 \times 10^4$  cells/cm<sup>2</sup>) on (PSS/PAH)<sub>n</sub> bilayers. a – cells on 12 bL; b – on 24 bL.

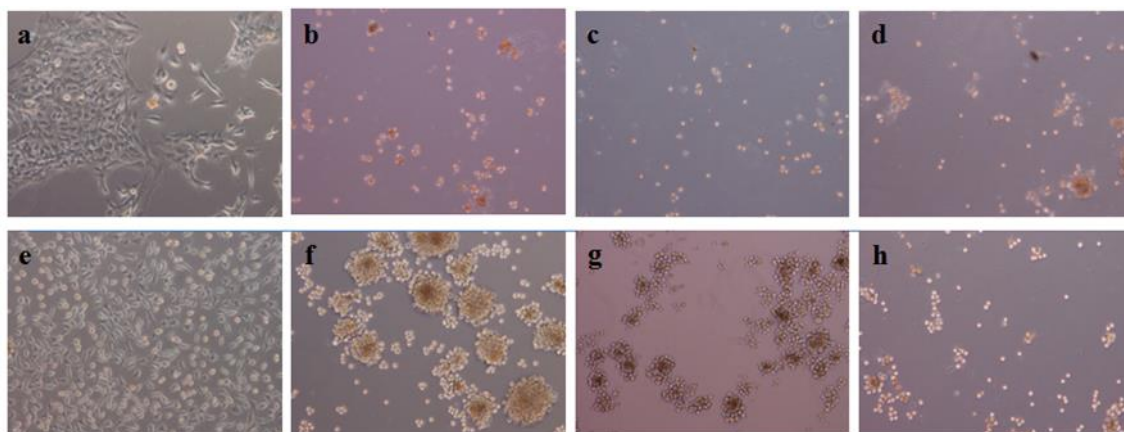


**Fig. S2.** Effect of surface treatment on growth of cells before film deposition. Phase contrast images of cells observed 2 days after seeding ( $1 \times 10^4$  cells/cm<sup>2</sup>) on (HA/PLL)<sub>n</sub> bilayers. a – 3T3 cells on a 12 bL surface with piranha treatment; b – 3T3 cells on a 24 bL surface with piranha treatment; c – 3T3 cells on a 24 bL surface with hellmanex-HCl treatment; d – 3T3 cells on a 24 bL surface with hellmanex-ultrasonication treatment; e – L929 cells on a 12 bL surface with piranha treatment; f – L929 cells on a 24 bL surface with piranha treatment; g – L929 cells on a 24 bL surface with hellmanex-HCl treatment; h – L929 cells on a 24 bL surface with hellmanex-ultrasonication treatment.

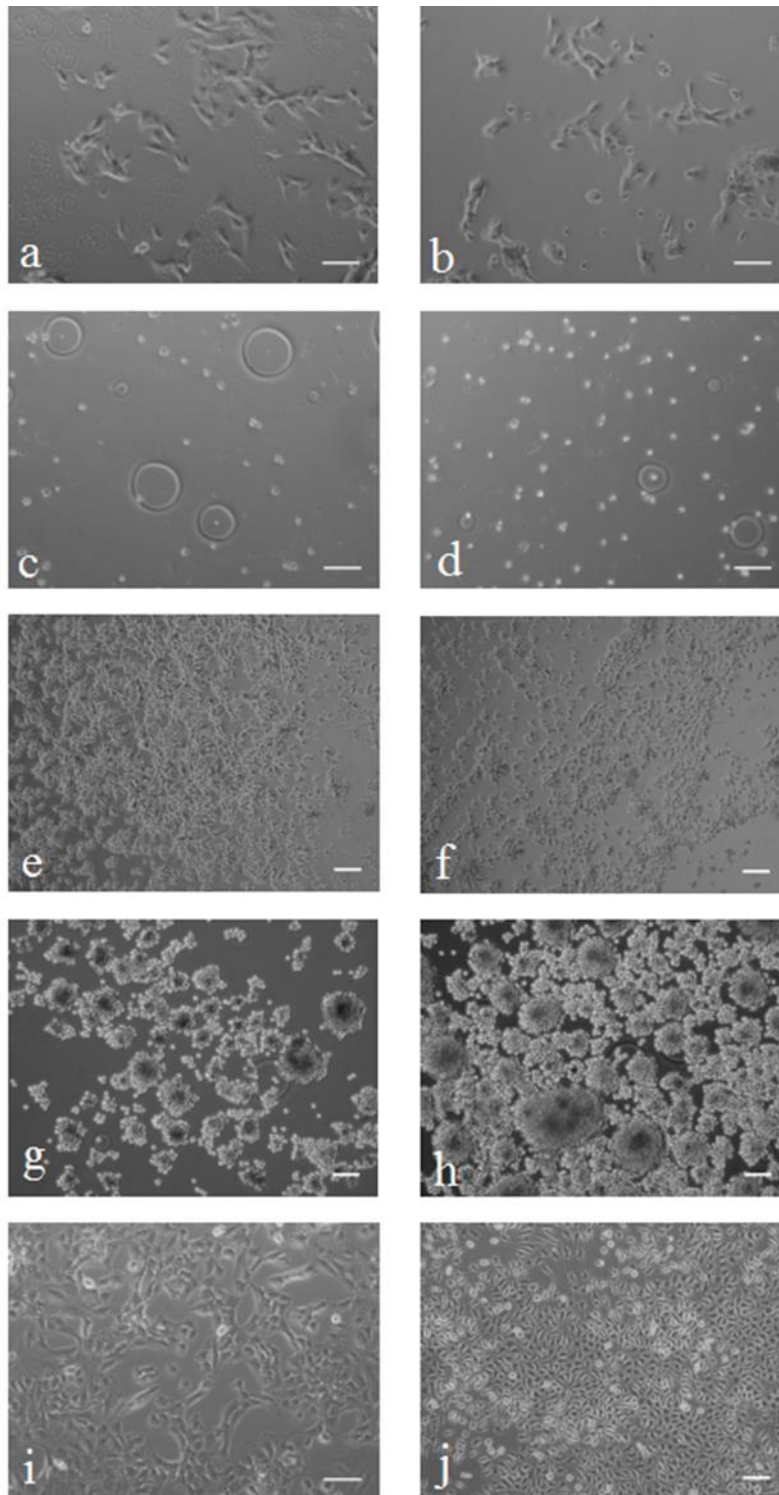


**Fig. S3:** Effect of fibronectin: Phase contrast images of cells grown on the (HA/PLL)<sub>n</sub> films.

a – 3T3 on 12bL with Fibronectin (F); b – 3T3 on 12bL without F;

c – 3T3 on 24bL with F; d – 3T3 on 24bL without F;

e – L929 on 12bL with F; f – L929 on 12bL without F;

g – L929 on 24bL with F; h – L929 on 24bL without F;

i – 3T3 on uncoated glass; j – L929 on uncoated glass. Scale – 100  $\mu$ m

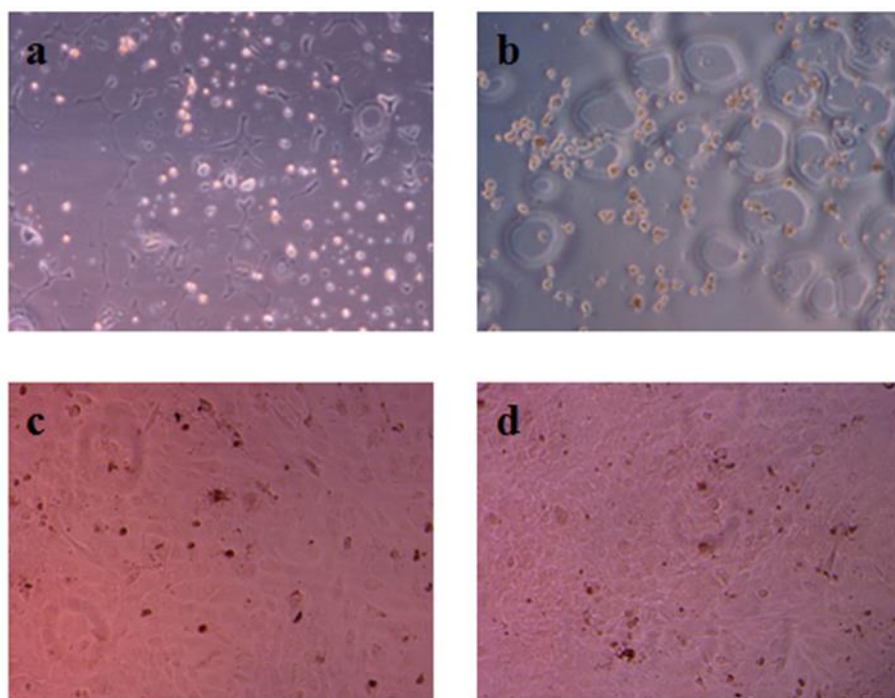


**Fig. S4.** Effect of serum on growth of cells on surfaces. Phase contrast images of cells in media without serum, observed 2 days after seeding ( $1 \times 10^4$  cells/cm<sup>2</sup>) on (HA/PLL)<sub>12</sub> bilayers. a – 3T3 cells on 24 bL; b – L929 cells on 24 bL; c – 3T3 cells on 12 bL; d – L929 cells on 12 bL

### A “cell-friendly” window for the interaction of cells with hyaluronic acid/poly-L-lysine multilayers

Narayanan Madaboosi,<sup>a,b</sup> Katja Uhlig,<sup>a</sup> Stephan Schmidt,<sup>a,c</sup> Anna S. Vikulina,<sup>d</sup> Helmuth Möhwald,<sup>b</sup> Claus Duschl,<sup>a</sup> Dmitry V. Volodkin<sup>a,d\*</sup>

<sup>a</sup> Fraunhofer Institute for Cell Therapy and Immunology, Branch Bioanalytics and Bioprocesses (Fraunhofer IZI-BB), Department Cellular Biotechnology & Biochips, Am Mühlenberg 13, 14476 Potsdam-Golm, Germany

<sup>b</sup> Max Planck Institute for Colloids and Interfaces, Am Mühlenberg 1, 14476 Potsdam-Golm, Germany

<sup>c</sup> Heinrich-Heine-Universität Düsseldorf, Institut für Organische und Makromolekulare Chemie, Universitätsstr.1, 40225 Düsseldorf, Germany

<sup>d</sup> School of Science and Technology, Nottingham Trent University, Clifton Lane, Nottingham NG11 8NS, United Kingdom

Corresponding author: Prof Assoc Dmitry V. Volodkin,  
Email: [dmitry.volodkin@ntu.ac.uk](mailto:dmitry.volodkin@ntu.ac.uk)